Activation of Frog (*Xenopus laevis*) Eggs by Inositol Trisphosphate. I. Characterization of Ca^{2+} Release from Intracellular Stores

WILLIAM B. BUSA,* JAMES E. FERGUSON,* SURESH K. JOSEPH,‡ JOHN R. WILLIAMSON,‡ and RICHARD NUCCITELLI*

*Department of Zoology, University of California, Davis, California 95616; and ‡Department of Biochemistry and Biophysics, School of Medicine, University of Pennsylvania, Philadelphia, Pennsylvania 19104

ABSTRACT Iontophoresis of inositol 1, 4, 5-trisphosphate into frog (*Xenopus laevis*) eggs activated early developmental events such as membrane depolarization, cortical contraction, cortical granule exocytosis, and abortive cleavage furrow formation (pseudocleavage). Inositol 1, 4-bisphosphate also triggered these events, but only at doses ~100-fold higher, whereas no level of fructose-1, 6-bisphosphate tested activated eggs. Using Ca^{2+}-selective microelectrodes, we observed that activating doses of inositol 1, 4, 5-trisphosphate triggered a Ca^{2+} release from intracellular stores that was indistinguishable from that previously observed at fertilization (Busa, W. B., and R. Nuccitelli, 1985, *J. Cell Biol.*, 100:1325–1329), whereas subthreshold doses triggered only a localized Ca^{2+} release at the site of injection. The subthreshold IP_3 response could be distinguished from the major Ca^{2+} release at activation with respect to their dose-response characteristics, relative timing, sensitivity to external Ca^{2+} levels, additivity, and behavior in the activated egg, suggesting that the *Xenopus* egg may possess two functionally distinct Ca^{2+} pools mobilized by different effectors. In light of these differences, we suggest a model for intracellular Ca^{2+} mobilization by sperm–egg interaction.

A transient increase in intracellular free Ca^{2+} concentration ($[Ca^{2+}]_i$)[1] accompanies fertilization in both invertebrate (8, 9, 23) and vertebrate eggs (4, 6, 16, 21), and considerable evidence suggests that such Ca^{2+} pulses provide the primary regulatory signal that triggers the initiation of development in the zygote (13, 18). The means by which sperm–egg interaction triggers intracellular Ca^{2+} release in the egg is unknown, but Ca^{2+}-induced Ca^{2+} release has been suggested to be involved (18, 22).

Recently, considerable evidence has accumulated that implicates the turnover of inositol lipids in the mobilization of intracellular Ca^{2+} seen in a variety of cell types during hormonal stimulation. In response to hormones such as acetylcholine, vasopressin, or platelet-derived growth factor, responsive cells such as pancreatic acinar cells, hepatocytes, or cultured fibroblasts, respectively, undergo a pronounced increase in the hydrolysis of the plasma membrane lipid, phosphatidylinositol-4, 5-bisphosphate (PIP_2), releasing into the cytosol the water-soluble product, inositol-1, 4, 5-trisphosphate (IP_3), which, in turn, can trigger Ca^{2+} release from intracellular stores in these and other cells (see references 1 and 2 for review). That hydrolysis of PIP_2, yielding IP_3, may also be the trigger for Ca^{2+} release in eggs at fertilization is suggested by recent observations on sea urchin eggs. Fertilization of these eggs triggers a rapid turnover of PIP_2 (24), and microinjection of IP_3 into the unfertilized egg elicits fertilization envelope elevation, presumably due to cortical granule exocytosis triggered by an increase in $[Ca^{2+}]_i$ (25).

In the present study, we demonstrate that iontophoresis of IP_3 activates several aspects of early development in the eggs of a vertebrate—the frog, *Xenopus laevis*—and triggers a transient Ca^{2+} release essentially indistinguishable from that which we have previously shown to accompany fertilization (4). Finally, we report initial studies using a novel double-barreled microelectrode to observe the localized response of $[Ca^{2+}]_i$ to subthreshold doses of IP_3, and suggest, based on these data, that the egg may contain two functionally distinct pools of mobilizable Ca^{2+}.

MATERIALS AND METHODS

Procurement and Handling of Gametes: *Xenopus laevis* eggs were obtained and treated as previously described (4). The nominally Ca^{2+}-free medium used in certain experiments, as specified below, was standard F1 solution (17), except that no Ca^{2+} was added, and Ca^{2+} contamination was controlled by adding 1 mM EGTA. The resulting free Ca^{2+} concentration, as determined with the Ca^{2+}-selective microelectrodes described below, was <0.1 μM. All other experiments were performed in standard F1.

[1] *Abbreviations used in this paper*: $[Ca^{2+}]_i$, intracellular free Ca^{2+} concentration; IP_2, inositol-1, 4-bisphosphate; IP_3, inositol-1, 4, 5-trisphosphate; pCa, negative log of free Ca^{2+} concentration; PIP_2, phosphatidylinositol-4, 5-bisphosphate.

Electrophysiological Recording and Iontophoresis: Measurements of $[Ca^{2+}]_i$ employing conventional single-barreled Ca^{2+}-selective microelectrodes were performed as previously described (4), except that Ca^{2+} microelectrode tips were bevelled (instead of broken) after filling but before dipping in the polyvinyl-chloride–gelled sensor, using a jet-stream microbeveller (19).

For studies of the local response of $[Ca^{2+}]_i$ to iontophoresis of IP_3, double-barreled microelectrodes were constructed. Commercial double-barreled capillary tubing (A-M Manufacturing, Spokane, WA) was pulled in a single stage on a vertical puller to yield typical double-barreled micropipets. The two barrels were then separated by gently forcing a razor blade's edge between them, beginning at the back end and advancing toward the tip. One barrel was then silanized as previously described (4) and used to construct a Ca^{2+}-selective microelectrode as described above. The two barrels were then rejoined with cyanoacrylate adhesive, using two micromanipulators and observing the tips at a magnification of 250. These electrodes functioned optimally when the two tips were left separated by 10–20 μm, and the results reported here are from such electrodes. After reassembly, the untreated barrel was loaded with the specified iontophoresis solution as described below.

All iontophoresis electrodes were backfilled with 1-mM solutions of either IP_3, inositol-1, 4-bisphosphate (IP_2), or fructose-1, 6-bisphosphate, as specified, in every case in 0.1 mM HEPES, pH 7.8. To conserve IP_3, no more than 2 μl of solution was used in an iontophoresis electrode. Electrical connection with this filling solution was made via an Ag/AgCl wire glued into the iontophoresis electrode. Negative current was injected between the iontophoresis electrode and bath ground using the constant current injection circuit of a Biodyne (Santa Monica, CA) AM-4 preamplifier, and current commands were supplied to the amplifier through a stimulus isolator (model 305, W-P Instruments, Inc., New Haven, CT) by an Anapulse stimulator (model 301, W-P Instruments, Inc.). The injected current was monitored at the current monitor output of the amplifier using an oscilloscope with a Tektronix digital waveform analyzer (model 5D10, Tektronix, Inc., Beaverton, OR), and both this oscilloscope and a chart recorder were used to record the Ca^{2+} electrode output.

Cell impalement with single-barreled iontophoresis electrodes was achieved with the aid of a custom-built piezoelectric advancer that rapidly advanced the electrode ~20 μm to achieve shallow impalement. Deep impalements were achieved by manually advancing the iontophoresis electrode ~100–200 μm beyond the initial shallow impalement using a micro-manipulator. During withdrawal from the egg, shallowly implanted electrodes (viewed under a dissecting microscope at 120×) emerged from the cell readily, whereas with deeply implanted electrodes, a substantial (~100 μm) length of the electrode shaft could be seen to emerge slowly from the adhering plasma membrane of this 1,300-μm-diam egg. Judged by this latter criterion, shallow impalements with the double-barreled electrode were only rarely possible; the impalements with such electrodes reported here are thus considered to have been deep.

All impalements with both Ca^{2+}-selective and iontophoretic electrodes were performed in the pigmented animal hemisphere of the eggs. All experiments were performed at room temperature, 21.5–23°C.

Preparation of IP_2 and IP_3: ^{32}P-labeled IP_2 and ^{32}P-labeled IP_3 used in the early studies reported here were prepared from human erythrocytes, and their purity was assessed by thin layer chromatography, as described elsewhere (7, 11). The IP_3 preparation ran as a single spot with the expected mobility, but the IP_2 displayed a minor (~10%) unidentified contaminant with a mobility different from that of IP_3. In later studies, commercially prepared IP_3 (Sigma Chemical Co., St. Louis, MO) was used with identical results.

Statistical Analysis: All averages are expressed as the mean ± SEM. Significance of differences between means was determined using the Student's t test for unpaired data. The criterion for significance was $P < 0.05$.

RESULTS

IP_3 Specifically Activates Xenopus Eggs

To determine the minimum doses of IP_2 or IP_3 necessary to activate eggs, a sequence of increasingly larger injections (as specified below), separated by 4-min intervals, was performed on each egg. This interval was chosen because repeated subthreshold IP_3 injections at 4-min intervals never activated eggs and, as we shall show below, the localized $[Ca^{2+}]_i$ increase elicited by a subthreshold IP_3 injection required ~4 min to return to the initial resting $[Ca^{2+}]_i$ level. The primary criteria used to score egg activation were a rapid, transient plasma membrane depolarization (the so-called activation potential), followed ~5 min later by contraction of the pigmented animal hemisphere toward the animal pole (cortical contraction). After removal of the electrodes, a subset of eggs was further observed for rotation within the vitelline envelope (reflecting cortical granule exocytosis) and abortive cleavage furrow formation (so-called pseudocleavage, typical of artificially activated eggs). In every instance, eggs which displayed an activation potential and cortical contraction also rotated and pseudocleaved. As reviewed in reference 10, all these events are typical of activated frog eggs.

For eggs shallowly impaled (see Materials and Methods) in the animal hemisphere with a single-barreled iontophoresis electrode, injection of as little as 0.32 nC from an IP_3-filled electrode (3.2 nA for 100 ms) triggered a rapid depolarization of the plasma membrane (Fig. 1) and cortical contraction, signaling egg activation. Using a sequence of 100-ms injections beginning at 3.2 nA and increasing by about this same value at each step, the minimum activating charge ranged from 0.32 to 1.6 nC, and averaged 0.84 ± 0.04 nC for nine eggs from three females. Assuming, as a first approximation, that all of the outward component of this charge was carried by IP_3 with a net molecular charge of −6, this would represent a mean activating dose of 0.73 fmol IP_3 per egg. This value is an upper limit only, however. The actual dosage of IP_3 delivered may have been as little as a fifth of this value, since transport numbers for iontophoresis of anions can be ≤0.1 (20), rather than the ideal value of 0.5 we have assumed here.

Eggs deeply impaled with the iontophoresis electrode required significantly more IP_3 to trigger their activation. Using a sequence of 33-nA injections of 0.1, 0.2, ... 1.0-s durations, the minimum activating charge ranged from 6.6 nC to 32.8 nC for ten eggs from three females, and averaged 18.0 ± 0.8 nC (significantly greater than the average activating charge of 0.84 nC for shallow injections; $P < 0.01$). In contrast with shallow IP_3 injections, which invariably triggered activation potentials either during or immediately after the 100-ms injection interval (Fig. 1), activation potentials after deep injections of IP_3 commenced an average of 9 ± 2 s ($n = 10$) after onset of the iontophoretic current.

To ensure that the activation elicited by IP_3 iontophoresis was specific for this compound and not due, for instance, to

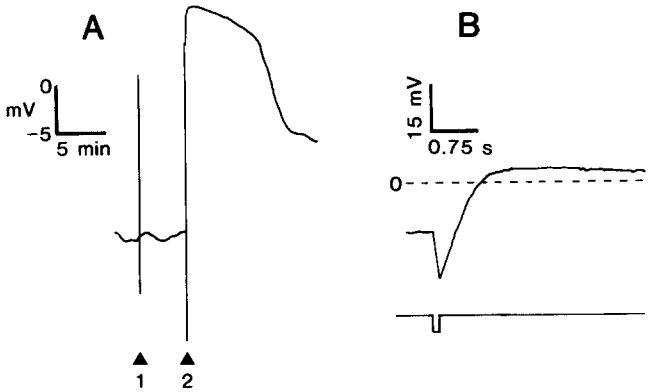

FIGURE 1 Tracings of membrane potential recordings from an egg activated by shallow iontophoresis of IP_3. (*A*) Chart recording. (*1*) 6.4 nA IP_3, 100 ms. (*2*) 9.6 nA IP_3, 100 ms. Note activation potential. This egg displayed a typical cortical contraction ~10 min after activation, and abortive cleavage furrow formation began 85 min after activation. (*B*) Oscilloscope recording of point *2* in Fig. 1*A*. Upper trace shows membrane potential (0 mV indicated by dashed line). Lower trace shows duration of the iontophoresis current. Activation potential begins sometime during the 100-ms injection.

some indirect effect of current injection, we tested the effect of iontophoresing fructose-1, 6-bisphosphate into shallowly impaled eggs. For seven eggs from two females, fructose-1, 6-bisphosphate injections of 131 nC (32.8 nA for 4 s) never elicited any sign of activation. In contrast, shallow injections of IP_2 did activate eggs, but only at much higher doses than those required with IP_3. Using sequential 33-nA injections of 0.5, 1.0, ... 3.0-s durations, the minimum activating charge ranged from 33 to 99 nC and averaged 60.9 ± 3.2 nC for seven eggs from three females. Based on a net molecular charge of −4 and transport number of 0.5, this represents an upper limit of 79 fmol IP_2 per egg, more than 100 times the average calculated dose of IP_3 required to trigger activation. We cannot rule out the likely possibility that this apparent activating effect of IP_2 was due to the minor contaminant detected in this preparation (see Materials and Methods).

IP_3-induced Activation Involves a Transient $[Ca^{2+}]_i$ Increase Identical to That Accompanying Fertilization

The ability of microinjected IP_3 to trigger fertilization envelope elevation in sea urchin eggs, as recently reported by Whitaker and Irvine (25), was presumed by them to be due to an IP_3-induced transient increase in $[Ca^{2+}]_i$. To determine whether a $[Ca^{2+}]_i$ increase accompanied IP_3-induced activation in *Xenopus* eggs, we used Ca^{2+}-selective microelectrodes to measure $[Ca^{2+}]_i$ directly during IP_3 iontophoresis. Fertilization of *Xenopus* eggs triggers an increase in $[Ca^{2+}]_i$ beginning (as detected by deeply impaling electrodes) ~1 min after the activation potential, rising over 2 min from an average resting level of 0.4 μM (pCa 6.4 [negative log of free Ca^{2+} concentration]) to a peak of 1.2 μM (pCa 5.9), and returning over 10 min to its initial value (4). As shown in Fig. 2, iontophoresis of a nonactivating dose of IP_3 (henceforth referred to as a sub-threshold dose) had no detectable effect on $[Ca^{2+}]_i$ measured ~275 μm from the site of iontophoresis (point *1* in Fig. 2), while an activating dose of IP_3 (here, 16 nC; point *2*) triggered a transient $[Ca^{2+}]_i$ increase from 0.29 μM (pCa 6.54) to 2.5 μM (pCa 5.6), indistinguishable from that previously observed to accompany fertilization. In three experiments with eggs from two females, activating injections of IP_3 triggered transient $[Ca^{2+}]_i$ increases from an average resting level of 0.25 μM (pCa 6.6 ± 0.1) to 1.58 μM (pCa 5.8 ± 0.2) as observed at a Ca^{2+}-selective microelectrode located >250 μm (along the egg surface) from the iontophoresis electrode. As we shall show below, the local $[Ca^{2+}]_i$ response to IP_3 injection begins almost immediately at the injection site; hence, the 31-s delay between iontophoresis and detection of the Ca^{2+} pulse in Fig. 2 reflects a propagation rate of 8.9 μm/s (here, at 22.5°C), in good agreement with the propagation rate of 9.7 ± 1.5 μm/s previously determined for the Ca^{2+} wave accompanying fertilization in these eggs (4).

Comparison of IP_3- and Ionophore-induced Ca^{2+} Release Using Double-Barreled Microelectrodes

As discussed above, the transient $[Ca^{2+}]_i$ increase seen in Fig. 2 and similar experiments is apparently identical to the propagated wave of $[Ca^{2+}]_i$ increase that we have previously shown to traverse the egg as a band of elevated free Ca^{2+} concentration at fertilization (4). To study separately the characteristics of the local response of $[Ca^{2+}]_i$ to injection of

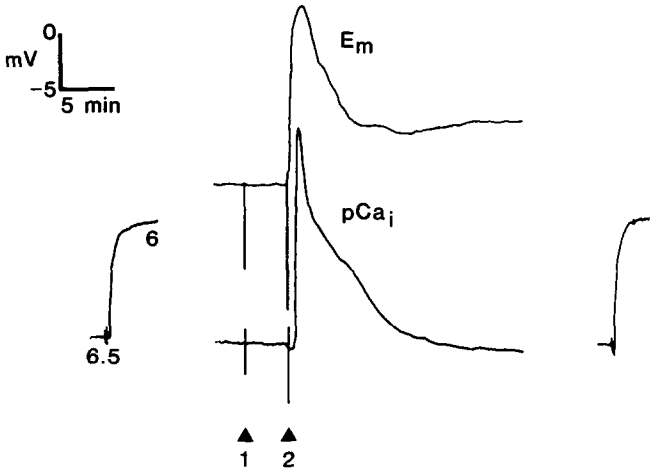

FIGURE 2 Tracings of membrane potential (E_m) and intracellular free Ca^{2+} (pCa_i) recordings from an egg activated by deep iontophoresis of IP_3. Traces at bottom left and right show Ca^{2+} electrode calibrations (pCa 6.5 and 6) before and after impalement. The Ca^{2+}-selective electrode and IP_3 iontophoresis electrode were separated by ~275 μm along the egg surface. (*1*) 32 nA IP_3, 100 ms. Note absence of detectable $[Ca^{2+}]_i$ response at this distance from the iontophoresis electrode. (*2*) 32 nA IP_3, 500 ms. The Ca^{2+} pulse accompanying activation is first detected at the Ca^{2+} electrode 31 s after onset of the iontophoresis current.

IP_3 and the (possibly distinct) global Ca^{2+} release which constitutes the propagated Ca^{2+} wave in *Xenopus* eggs, we have employed a novel double-barreled microelectrode incorporating both a Ca^{2+}-selective microelectrode and an IP_3 iontophoresis electrode whose tips are separated by no more than 20 μm. As shown in Fig. 3*A*, passage of current through the iontophoresis barrel (here, filled with IP_2 solution) elicited a transient spike artifact in the Ca^{2+} electrode output due, presumably, to charging of the latter electrode's capacitance during current ejection from the nearby iontophoresis electrode. Similar artifacts, requiring ~4 s to recover, were consistently observed whether the electrode tip was in a cell (Fig. 3*A*, points *1–5*) or simply immersed in buffer (Fig. 3*A*, point *6*) when the iontophoresis electrode was filled with IP_2 (which, as discussed above, did not trigger activation at the doses used here). No longer-lasting response to IP_2 iontophoresis was observed intracellularly, indicating that IP_2 at the doses used here did not trigger detectable Ca^{2+} release in the egg. The typical Ca^{2+} pulse observed here during activation with the Ca^{2+} ionophore, A23187 (2 μM), demonstrated that the Ca^{2+} electrode could detect $[Ca^{2+}]_i$ changes.

In contrast with the absence of an observable local $[Ca^{2+}]_i$ response to IP_2 iontophoresis, iontophoresis of subthreshold doses of IP_3 into the unactivated egg elicited both the initial current-flow artifact discussed above as well as a further, transient increase in $[Ca^{2+}]_i$ requiring ~4 min to recover to the initial resting value of $[Ca^{2+}]_i$ (Fig. 3*B*, *points 2–5*). This latter response was only observed intracellularly and never when the double-barreled electrode was simply immersed in buffer (Fig. 3*B*, points *1* and *10*), indicating that it accurately reflects a localized increase of $[Ca^{2+}]_i$ in response to IP_3 injection. Injection of increasing amounts of IP_3 demonstrated a typical dose-response relationship by $[Ca^{2+}]_i$ in both the unactivated (Fig. 3*B*, points *2–5*) and activated egg (points *7–9*) with larger $[Ca^{2+}]_i$ increases in response to larger doses of IP_3. As illustrated in Fig. 2, transient $[Ca^{2+}]_i$ increases were

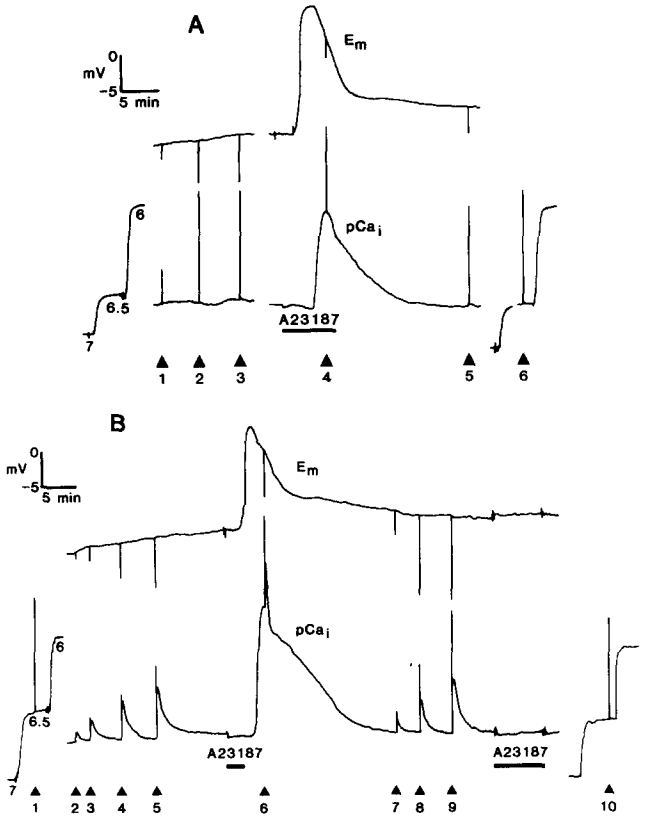

FIGURE 3 Tracings of membrane potential (E_m) and intracellular free Ca^{2+} (pCa_i) recordings from eggs iontophoresed with IP_2 (*A*) and IP_3 (*B*) using the double-barreled electrode (see text). Traces at bottom left and right in each figure show Ca^{2+} electrode calibrations (pCa 7, 6.5, and 6) before and after impalement. During the intervals indicated by the bars, 2 μM A23187 was present in the bathing medium. (*A*) IP_2 iontophoresis, 30 nA current for the following intervals: (*1*) 20 ms. (*2*) 60 ms. (*3*) 100 ms. (*4*) 40 ms, injected at the height of Ca^{2+} pulse accompanying A23187-induced activation. (*5*) 40 ms. (*6*) 100 ms, injected into calibration buffer after withdrawal from egg. (*B*) IP_3 iontophoresis, 30 nA current for the following intervals: (*1*) 100 ms, injected into calibration buffer before cell impalement. (*2*) 10 ms. (*3*) 20 ms. (*4*) 40 ms. (*5*) 70 ms. (*6*) 150 ms, injected at height of Ca^{2+} pulse accompanying A23187-induced activation. (*7*) 20 ms. (*8*) 70 ms. (*9*) 150 ms. (*10*) 100 ms, injected into calibration buffer after withdrawal from egg.

never observed in response to nonactivating doses of IP_3 when the Ca^{2+}-selective microelectrode and iontophoresis electrode were widely separated along the surface of this 1.3-mm-diam egg, indicating the local and nonpropagated nature of the $[Ca^{2+}]_i$ response to subthreshold IP_3 injections shown in Fig. 3*B*.

Two observations apparent in Fig. 3*B* suggest the possibility that the IP_3-sensitive Ca^{2+} pool in the *Xenopus* egg is functionally distinct from the major pool of Ca^{2+} mobilized (here, by A23187) to yield the propagated Ca^{2+} wave at activation. First, when the egg was activated by brief treatment with 2 μM A23187, an IP_3-induced Ca^{2+} release could still be triggered even at the peak of the ionophore-induced Ca^{2+} release (Fig. 3*B*, point *6*), although in this case its recovery was always much more rapid than that seen in the unactivated egg. Second, after recovery of $[Ca^{2+}]_i$ back to its basal level after activation with ionophore, IP_3 injection still elicited normal (albeit, slightly reduced) local $[Ca^{2+}]_i$ increases (Fig. 3*B*, points *7–9*), even though additional treatments with A23187 failed to trigger further major $[Ca^{2+}]_i$ increases. The experiment of Fig. 3 was repeated with three eggs from three females, with identical results.

$[Ca^{2+}]_i$ Increases during IP_3 Injection and Activation Reflect Release of Ca^{2+} from Intracellular Stores

To determine the source (i.e., intracellular store or extracellular medium) of the Ca^{2+} released into the cytosol either in response to a subthreshold IP_3 injection or during the major Ca^{2+} pulse accompanying activation, we studied the response of $[Ca^{2+}]_i$ in eggs bathed in nominally Ca^{2+}-free medium (Fig. 4). These experiments were complicated, however, by the destabilizing effect of Ca^{2+}-free media on the egg plasma membrane, as indicated by both a decrease in membrane potential under Ca^{2+}-free conditions (Fig. 4*A*) and, occasionally, by a clearing of pigment from around the electrode impalement sites (this was observed in the egg used in Fig. 4*B*, but not in that of Fig. 4*A*). For the eight eggs (from five females) studied, two failed to display a typical local $[Ca^{2+}]_i$ response to subthreshold injections of IP_3 (illustrated in Fig. 4*B*),[2] whereas six showed little or no difference between the response in Ca^{2+}-free and Ca^{2+}-containing media (Fig. 4*A*). Additionally, even eggs that displayed a decreased IP_3 response in Ca^{2+}-free F1 could still be activated by large IP_3 injections, and still displayed a Ca^{2+} pulse of normal magnitude at activation (Fig. 4*B*, point *6*). For control experiments in which both the Ca^{2+}-selective and indifferent electrodes dimpled the egg but did not impale it, extracellular Ca^{2+} levels of <pCa 6.5 were recorded within 4 min after Ca^{2+}-containing F1 was changed to Ca^{2+}-free medium, demonstrating that the jelly layer of these eggs did not retain high levels of free Ca^{2+} near the cell surface. We therefore treated the eggs discussed here with Ca^{2+}-free medium for a minimum of 5 min before initiating iontophoresis. Thus, these studies suggest that both the subthreshold IP_3 response and the major Ca^{2+} pulse at activation are due to a release of sequestered Ca^{2+} from some intracellular store(s). It appears, however, that under conditions in which cytosolic Ca^{2+} might leak out of the cell (due to impalement damage in Ca^{2+}-free medium), the IP_3-sensitive intracellular Ca^{2+} pool can be partially depleted, even under conditions that apparently do not decrease the magnitude of the major Ca^{2+} pulse at activation.

DISCUSSION

New Findings

Using Ca^{2+}-selective microelectrodes, we have directly demonstrated for the first time with germ cells what has previously been demonstrated with somatic cells from a variety of vertebrates, i.e., that intracellular Ca^{2+} stores can be specifically mobilized, leading to transient increases in $[Ca^{2+}]_i$, by the intracellular application of very small doses of IP_3. This is also the first demonstration that IP_3 can mobilize intracellular Ca^{2+} stores in intact cells, since all previous studies in which Ca^{2+} release was directly measured have utilized permeabilized cell models to facilitate delivery of exogenously applied

[2] The lack of response to subthreshold IP_3 injection in Ca^{2+}-free medium illustrated here has only been observed in two eggs. Unfortunately, we did not perform prior controls using Ca^{2+}-containing media with these two cells (as was done in the experiment of Fig. 4*A* and all other experiments).

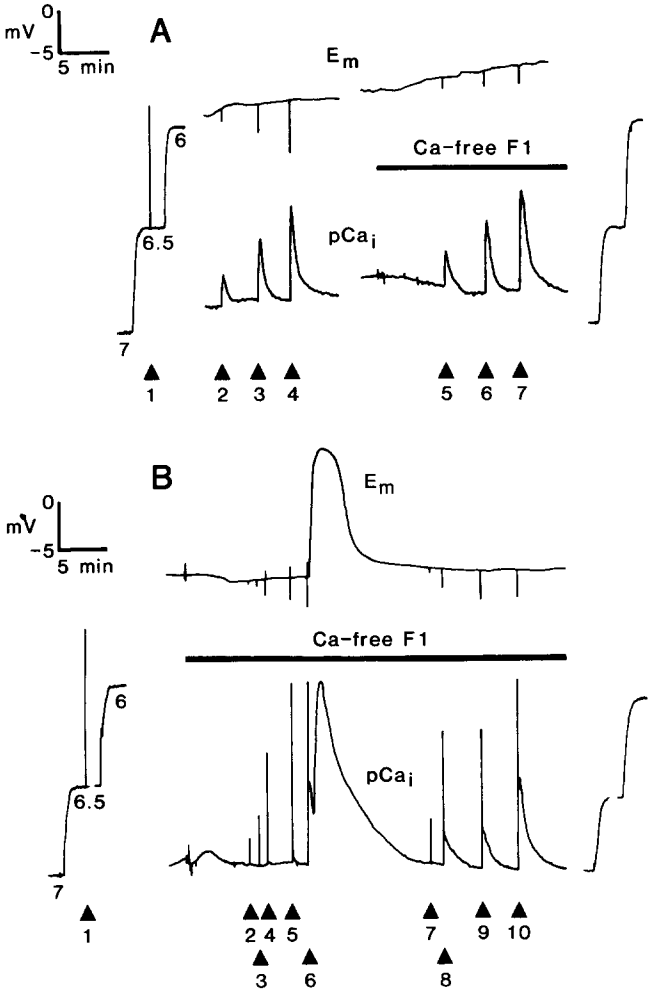

FIGURE 4 Tracings of membrane potential (E_m) and intracellular free Ca^{2+} (pCa_i) recordings during iontophoresis with IP_3 of eggs bathed in complete F1, containing 0.25 mM Ca^{2+}, or in nominally Ca^{2+}-free F1 with 1 mM EGTA (indicated by bar). Traces at bottom left and right in each figure show Ca^{2+} electrode calibrations (pCa *7*, *6.5*, and *6*) before and after impalement. (*A*) Typical result displayed by six of eight eggs, illustrating lack of dependence on external Ca^{2+}. All injections used a 30-nA iontophoresis current for the following intervals: (*1*) 100 ms, injected into calibration buffer before impalement. (*2*) 10 ms. (*3*) 20 ms. (*4*) 35 ms. (*5–7*) Same as 2–4, respectively, but after changing bathing medium to Ca^{2+}-free F1. (*B*) Response displayed by two of eight eggs, illustrating partial dependence on external Ca^{2+}. All injections were 30 nA for the following intervals: (*1*) 100 ms, injected into calibration buffer before impalement. (*2*) 10 ms. (*3*) 20 ms. (*4*) 50 ms. (*5*) 100 ms. (*6*) 300 ms. Note resolution of the local IP_3 response from the major Ca^{2+} pulse accompanying activation. (*7*) 20 ms. (*8*) 75 ms. (*9*) 100 ms. (*10*) 300 ms.

IP_3 to its intracellular target(s) (see references 1 and 2 for review). Since cell permeabilization inevitably leads to uncontrollable and nonphysiological changes in the internal milieu, with potentially confounding effects, the present demonstration of IP_3-induced Ca^{2+} release in intact cells is an important addition to the study of IP_3-mediated regulation of $[Ca^{2+}]_i$.

Our present report also demonstrates for the first time that vertebrate eggs can be triggered to initiate the early events of development by intracellular application of low doses of IP_3 (presumably due to the transient increase in $[Ca^{2+}]_i$ just discussed), thus confirming and expanding upon the recent report by Whitaker and Irvine (25) that microinjection of IP_3 activates sea urchin eggs (see Noted Added in Proof). These authors used as the criteria for egg activation the elevation of the fertilization envelope (reflecting cortical granule exocytosis) and the increase in intracellular fluorescein fluorescence which signals an increase in intracellular pH (another event accompanying egg activation; see reference 3 for review). In our studies, we have used an extensive set of criteria, including the activation potential (a transient depolarization of the plasma membrane), cortical contraction, cortical granule exocytosis (reflected by egg rotation within the vitelline envelope), and the abortive cleavage furrow formation (pseudocleavage) which commonly accompanies artificial activation of unfertilized frog eggs. Thus, the present study demonstrates that a wide variety of processes that normally comprise the early development of the zygote are all triggered by IP_3. In light of the previous demonstration that fertilization triggers a dramatic activation of PIP_2 hydrolysis in the sea urchin egg (24), these findings provide compellingly suggestive evidence that Ca^{2+}-mediated developmental activation of eggs may be triggered at fertilization by the generation of IP_3. It remains to be demonstrated directly that fertilization triggers a sufficient increase in cytosolic IP_3 concentration in any egg to elicit the responses seen with artificial applications of IP_3.

Characteristics of the Subthreshold IP_3-induced Ca^{2+} Release and the Ca^{2+} Pulse Accompanying Activation

Development of the double-barreled IP_3-iontophoresis/Ca^{2+}-measurement electrode has enabled us to begin the in vivo characterization of the mobilizable Ca^{2+} pool(s) responsible for the transient $[Ca^{2+}]_i$ increase accompanying the activation of *Xenopus* eggs. As shown in Fig. 4 (*A* and *B*), both the localized Ca^{2+} release triggered by IP_3 iontophoresis, as well as the major $[Ca^{2+}]_i$ increase at activation, are observable in eggs in Ca^{2+}-free medium, suggesting that both responses arise from the release into the cytosol of Ca^{2+} sequestered in some intracellular store(s). Several lines of evidence suggest that the localized IP_3-triggered $[Ca^{2+}]_i$ response documented in the present study and the global Ca^{2+} wave at activation (4) arise from the activities of functionally (and, perhaps, structurally) distinct Ca^{2+} pools. First, local IP_3-induced Ca^{2+} release can be demonstrated in either the unactivated or activated egg; in contrast, the ionophore-triggered Ca^{2+} pulse can only be elicited in the unactivated egg (Fig. 3*B*). In this respect, ionophore- (but not IP_3-) triggered Ca^{2+} release coincides with the presence of cortical endoplasmic reticulum–plasma membrane junctions in the *Xenopus* egg, which have been implicated in $[Ca^{2+}]_i$ regulation (4a, 5, 15), since these junctions are numerous in the unactivated egg but apparently disappear within 30–60 s of the completion of cortical granule exocytosis (15). Secondly, as seen in Fig. 4*B* (point *6*), the local IP_3 response (even in the absence of external Ca^{2+}) and the major Ca^{2+} pulse that it elicits can be temporally separated at a discrete site in the cytoplasm. Further, even when the IP_3-sensitive store is partially depleted, a major Ca^{2+} pulse of normal magnitude can still be observed to accompany activation. Interestingly, while the egg in Fig. 4*B* failed to respond to a 3-nC injection of IP_3 before activation, it responded normally to this same dose after the major Ca^{2+} pulse accompanying activation (compare points *5* and *9*), suggesting the

possibility that the Ca^{2+} released by the major pulse may have partially recharged the IP_3-sensitive store. Finally, even at the peak of the $[Ca^{2+}]_i$ transient elicited by A23187, a further incremental increase in $[Ca^{2+}]_i$ can still be achieved by injection of IP_3 (Fig. 3*B*). All of these observations are consistent with the possibility that the unactivated *Xenopus* egg possesses at least two functionally distinct mobilizable Ca^{2+} pools—one which can be specifically triggered to release Ca^{2+} into the cytosol in response to IP_3 and which survives activation functionally intact, and a second pool mobilized, for example, by the same sort of Ca^{2+}-induced Ca^{2+} release previously observed in both skeletal (12) and cardiac (14) muscle fibers, which might either be disassembled at activation or else simply fail to recharge. Efforts to test this two pool hypothesis are currently in progress.

If the two pool model proves correct, the following sequence of events might account for the behavior of $[Ca^{2+}]_i$ observed at fertilization in the frog egg. Sperm–egg interaction activates a local (at the sperm entry site) hydrolysis of PIP_2, releasing sufficient IP_3 into the cortical cytosol to elicit a local increase in $[Ca^{2+}]_i$ via Ca^{2+} release from the IP_3-sensitive pool. This local response, in turn, may then trigger a more extensive Ca^{2+}-induced Ca^{2+} release from the second (presumably IP_3-insensitive) pool, which would propagate across the egg via further Ca^{2+}-induced Ca^{2+} release (as previously suggested by Gilkey et al. [16]), thus giving rise to the Ca^{2+} wave we have previously documented with this egg. The principal role of this latter release is presumably to effect this propagated Ca^{2+} wave (observed, to date, in the eggs of four species [4, 8, 9, 16], but not in any somatic cell type) to protect against polyspermy by triggering the propagated exocytosis of the cortical granules. It may thus be of no further utility (and is therefore inactivated) after the initiation of development, leaving only the IP_3-sensitive Ca^{2+} pool which appears to be a rather common feature of somatic cells. This model differs from that previously proposed for the activating sea urchin egg by Whitaker and Irvine (25), who envisioned "... a mechanism in which IP_3-stimulated calcium release and calcium-stimulated IP_3 production cooperate to produce a wave of calcium release which propagates through the egg cytoplasm," in that it substitutes Ca^{2+}-induced Ca^{2+} release for Ca^{2+}-stimulated IP_3 production as the mechanism responsible for propagation of the Ca^{2+} wave beyond the sperm entry site. Both models, however, propose IP_3 production via PIP_2 hydrolysis as the proximate mechanism coupling sperm/egg interaction with the initial mobilization of intracellular Ca^{2+}. While these two models are not mutually exclusive, and might even simply reflect species differences, it is important to attempt to distinguish between them, as we are presently doing.

The notion that a cortically located Ca^{2+} pool (e.g., the cortical endoplasmic reticulum forming junctions with the plasma membrane) which exhibits Ca^{2+}-induced Ca^{2+} release may be responsible for the propagated Ca^{2+} wave at activation is in keeping with our observation that 20-fold more IP_3 is required to trigger activation when injected deeply (as opposed to shallowly) into the egg. If the local $[Ca^{2+}]_i$ increase induced by IP_3 triggers the major Ca^{2+} pulse via Ca^{2+}-induced Ca^{2+} release, as we have suggested, then the depth dependence of the IP_3 dose required to trigger activation could reflect the necessity for the IP_3-triggered $[Ca^{2+}]_i$ increase to reach these cortical targets. Larger doses of IP_3 elicit larger local $[Ca^{2+}]_i$ increases (Fig. 3), which, by diffusion, should involve larger volumes of cytosol. According to our model, then, deeply injected IP_3 should only trigger a global Ca^{2+} wave when the local $[Ca^{2+}]_i$ increase it elicits can reach the egg cortex.

This work was supported by National Science Foundation grant PCM 8118174 and National Institutes of Health grant KO4 HD00470 to Dr. Nuccitelli.

Received for publication 26 February 1985.

Note Added in Proof: While this paper was in press, it was reported that microinjection of IP_3 triggers activation of mature *Xenopus* oocytes (Picard, A., F. Giraud, F. Le Bouffant, F. Sladeczek, C. Le Peuch, and M. Dorée, 1985, *FEBS [Fed. Eur. Biochem. Soc.] Lett.*, 182:446–450).

REFERENCES

1. Berridge, M. J. 1984. Inositol trisphosphate and diacylglycerol as second messengers. *Biochem. J.* 220:345–360.
2. Berridge, M. J., and R. F. Irvine. 1984. Inositol trisphosphate, a novel second messenger in cellular signal transduction. *Nature (Lond.).* 312:315–321.
3. Busa, W. B., and R. Nuccitelli. 1984. Metabolic regulation via intracellular pH. *Am. J. Physiol.* 246:R409–R438.
4. Busa, W. B., and R. Nuccitelli. 1985. An elevated free cytosolic Ca^{2+} wave follows fertilization in eggs of the frog. *Xenopus laevis. J. Cell Biol.* 100:1325–1329.

4a. Campanella, C., P. Andreuccetti, C. Taddei, and R. Talevi. 1984. The modifications of cortical endoplasmic reticulum during in vitro maturation of *Xenopus laevis* oocytes and its involvement in cortical granule exocytosis. *J. Exp. Zool.* 229:283–293.

5. Charbonneau, M., and R. D. Grey. 1984. The onset of activation responsiveness during maturation coincides with the formation of the cortical endoplasmic reticulum in oocytes of *Xenopus laevis. Dev. Biol.* 102:90–97.
6. Cuthbertson, K. S. R., D. G. Whittingham, and P. H. Cobbold. 1981. Free Ca^{2+} increases in exponential phases during mouse oocyte activation. *Nature (Lond.).* 294:754–756.
7. Downes, C. P., M. C. Mussat, and R. H. Michell. 1982. The inositol trisphosphate phosphomonoesterase of the human erythrocyte membrane. *Biochem. J.* 203:169–177.
8. Eisen, A., D. P. Kiehart, S. J. Wieland, and G. T. Reynolds. 1984. Temporal sequence and spatial distribution of early events of fertilization in single sea urchin eggs. *J. Cell Biol.* 99:1647–1654.
9. Eisen, A., and G. T. Reynolds. 1984. Calcium transients during early development in single starfish *(Asterias forbesi)* oocytes. *J. Cell Biol.* 99:1878–1882.
10. Elinson, R. P. 1980. The amphibian egg cortex in fertilization and early development. *In* The Cell Surface: Mediator of Developmental Processes. S. Subtelny and N. K. Wessells, editors. Academic Press, Inc., New York. 217–234.
11. Emillson, A., and R. Sundler. 1984. Differential activation of phosphatidylinositol deacylation and a pathway via diphosphoinositide in macrophages responding to zymosan and ionophore A23187. *J. Biol. Chem.* 259:3111–3116.
12. Endo, M. 1977. Calcium release from the sarcoplasmic reticulum. *Physiol. Rev.* 57:71–108.
13. Epel, D. 1980. Experimental analysis of the role of intracellular calcium in the activation of the sea urchin egg at fertilization. *In* The Cell Surface: Mediator of Developmental Processes. S. Subtelny and N. K. Wessels, editors. Academic Press, Inc., New York. 169–185.
14. Fabiato, A., and F. Fabiato. 1979. Calcium and cardiac excitation-contraction coupling. *Ann. Rev. Physiol.* 41:473–484.
15. Gardiner, D. M., and R. D. Grey. 1983. Membrane junctions in *Xenopus* eggs: their distribution suggests a role in calcium regulation. *J. Cell Biol.* 96:1159–1163.
16. Gilkey, J. C., L. F. Jaffe, E. B. Ridgway, and G. T. Reynolds. 1978. A free calcium wave traverses the activating egg of the medaka. *Oryzias latipes. J. Cell Biol.* 76:448–466.
17. Hollinger, T. G., and G. L. Corton. 1981. Artificial fertilization of gametes from the South African clawed frog, *Xenopus laevis. Gamete Res.* 3:45–57.
18. Jaffe, L. F. 1980. Calcium explosions as triggers of development. *Ann. NY Acad. Sci.* 339:86–101.
19. Ogden, T. E., M. C. Citron, and R. Pierantoni. 1978. The jet stream microbeveler: an inexpensive way to bevel ultrafine glass micropipettes. *Science (Wash. DC).* 201:469–470.
20. Purves, R. D. 1981. Microelectrode Methods for Intracellular Recording and Ionophoresis. Academic Press, Inc., London. 146 pp.
21. Ridgway, E. B., J. C. Gilkey, and L. F. Jaffe. 1977. Free calcium increases explosively in activating medaka eggs. *Proc. Nat. Acad. Sci. USA.* 74:623–627.
22. Schackmann, R. W., E. M. Eddy, and B. M. Shapiro. 1978. The acrosome reaction of *Strongylocentrotus purpuratus* sperm. Ion requirements and movements. *Dev. Biol.* 65:483–495.
23. Steinhardt, R., R. Zucker, and G. Shatten. 1977. Intracellular calcium release at fertilization in the sea urchin egg. *Dev. Biol.* 58:185–196.
24. Turner, P. R., M. P. Sheetz, and L. A. Jaffe. 1984. Fertilization increases the polyphosphoinositide content of sea urchin eggs. *Nature (Lond.).* 310:414–415.
25. Whitaker, M., and R. F. Irvine. 1984. Inositol 1, 4, 5-trisphosphate microinjection activates sea urchin eggs. *Nature (Lond.).* 312:636–639.